Mon. Not. R. Astron. Soc. **000**, 1–?? () Printed 10 December 2014 (MN LATEX style file v2.2)

A NuSTAR observation of the fast symbiotic nova V745 Sco in outburst

M. Orio [1,2⋆], V. Rana[3]†, K. L. Page[4]‡, J. Sokoloski[5]§, F. Harrison[3]¶
[1] *INAF–Osservatorio di Padova, vicolo dell' Osservatorio 5, I-35122 Padova, Italy*
[2] *Department of Astronomy, University of Wisconsin, 475 N. Charter Str., Madison WI 53704*
[3] *Cahill Center for Astronomy and Astrophysics, California Institute of Technology, Pasadena, CA 91125, USA*
[4] *Department of Physics and Astronomy, University of Leicester, Leicester, LE1 7RH, UK*
[5] *Columbia Astrophysics Laboratory, Columbia University, 550 West 120th Street, New York, NY 10027, USA*

arXiv:1412.2088v2 [astro-ph.HE] 9 Dec 2014

Accepted . Received; in original form

ABSTRACT
The fast recurrent nova V745 Sco was observed in the 3-79 keV X-rays band with *NuSTAR* 10 days after the optical discovery. The measured X-ray emission is consistent with a collisionally ionized optically thin plasma at temperature of about 2.7 keV. A prominent iron line observed at 6.7 keV does not require enhanced iron in the ejecta. We attribute the X-ray flux to shocked circumstellar material. No X-ray emission was observed at energies above 20 keV, and the flux in the 3-20 keV range was about 1.6 $\times$ 10^{-11} erg cm^{-2} s^{-1}. The emission measure indicates an average electron density of order of 10^7 cm^{-3}. The X-ray flux in the 0.3-10 keV band almost simultaneously measured with *Swift* was about 40 times larger, mainly due to the luminous central supersoft source emitting at energy below 1 keV. The fact that the *NuSTAR* spectrum cannot be fitted with a power law, and the lack of hard X-ray emission, allow us to rule out Comptonized gamma rays, and to place an upper limit of the order of 10^{-11} erg cm^{-2} s^{-1} on the gamma-ray flux of the nova on the tenth day of the outburst.

Key words: binaries: close, stars, white dwarfs, X-rays: stars

1 INTRODUCTION

Classical novae in outburst are very luminous X-ray sources for two reasons. One source of X-ray emission is the very hot white dwarf, burning hydrogen in a shell which is covered by only a thin atmosphere. In most novae the ejecta become transparent to X-rays before hydrogen burning has been completely quenched, so the X-ray emission is extremely soft, peaking below 1 keV, and very luminous, usually exceeding 10^{37} erg s^{-1} and often reaching a few times 10^{38} erg s^{-1} (see Orio 2012, and numerous references therein). In this work we deal with the second important source of X-ray emission, the nova ejecta. X-ray emission due to photoionization by the extremely hot central source cannot be completely ruled out, but most nova shells appear to contain collisionally ionized plasma, as expected from internal shocks (e.g. Metzger et al. 2014), even at late post-outburst phases (e.g. Rohrbach et al. 2009; Orio et al. 2013; Tofflemire et al. 2013), or in symbiotic novae because the nova wind impacts a previous red giant wind. This second phenomenon occurs in the early phases of the outburst (a typical case is RS Oph, see Nelson et al. 2008). The energy range of X-ray emission observed from the ejected nebula varies by orders of magnitude in different novae. The hard X-ray emission peaked in the third week after the eruption for V382 Vel (Mukai & Ishida 2001), after a week for RS Oph (Sokoloski et al. 2006), and after only 5 days for V838 Her (Lloyd et al. 1992).

In the last four years, GeV gamma rays have been detected in a handful of very luminous novae leaving open the possibility that all other novae may be gamma ray sources at a level below the luminosity detection threshold of Fermi (which is of the order of 10^{36} erg s^{-1} at a few kpc distance). For the symbiotic nova V407 Cyg, the gamma rays were attributed to pion decay, resulting from proton-proton interactions in the thick red giant wind in which particles are accelerated by of the nova outflows (Abdo et al. 2010), although Martin & Dubus (2013) favored instead a "leptonic origin", like in the other novae detected with Fermi (N Sco 2012, N Mon 2012, V339 Del, and V1369 Cen). In all these cases the gamma ray flux was attributed to a combina-

⋆ E-mail:marina.orio@oapd.inaf.it
†
‡
§
¶

© RAS

tion of inverse Compton scattering with low energy photons, and bremsstrahlung, when the electrons are accelerated in strong shocks in the circumstellar medium (see Ackerman et al. 2014 and references therein). A question that naturally arises is whether the hard X-ray emission of novae in outburst originates in the same medium, and from the same mechanisms, as the gamma ray emission. The X-rays may be due to Compton downscattering of gamma rays (see for instance Livio et al. 1992). The X-ray flux would then increase with energy, so it is important to monitor the hard X-ray window. The hard X-rays may also be due to a later phase in the evolution and cooling of the same shocked circumstellar plasma where the gamma rays originated. Hard X-rays were already detected from V745 Sco with *Swift* almost at the same time as the gamma ray emission (Page et al. 2014), but the range above 10 keV was not observed, and this nova evolves very rapidly.

Recent observations at radio wavelengths indicate that the mass outflow from novae is not a smooth phenomenon, and that new episodes of mass ejection may occur long after maximum (e.g. Nelson et al. 2014). In this scenario, a faster nova wind at some point may collide into a slower, initial nova wind, giving rise to a new burst of X-ray emission. Hard X-rays may also be associated with bipolar outflows (e.g. RS Oph, Sokoloski et al. 2008; Nelson et al. 2008). Finally, it has been speculated that hard X-rays offer diagnostics of the origin of mass outflows. They would be associated with outflow from the white dwarf in an early outburst phase, as opposed to large mass loss occurring later from the secondary (Williams 2013). Williams (2013) noted that in the X-ray spectra of V382 Vel Orio et al. (2001), and later Ness et al. (2005), did not detect iron lines, and suggested that the X-ray flux is emitted in the same ejecta as the optical "He/N spectrum", while the "Fe II" emission region is instead due to an outflow from the secondary, occurring without generating any X-ray flux. If the X-ray emitting gas is from the WD, iron lines should not be detectable. However, we do know that at least RS Oph had a clear iron emission feature, at least immediately after the outburst (Sokoloski et al. 2006; Bode et al. 2006).

Because of all these reasons, it is crucial to monitor X-rays from novae since the beginning of the eruption, in order to understand when the hard X-ray emission starts and whether there is a single emission region for the gamma and hard X-rays. The *NuSTAR* satellite is ideal for following the early X-ray emission of a nova shell, because of its broad energy range up to 79 keV and its excellent sensitivity in the iron lines region around 7 keV.

2 A REMARKABLE RECURRENT NOVA

V745 Sco is a remarkably fast nova, and one of only a handful of recurrent novae (RN) with giant secondaries (Duerbeck 1989; Sekiguchi et al. 1990; Williams et al. 1991). An orbital period of 510±20 days has been proposed (Schaefer 2009), but it has not been confirmed by OGLE data (Mróz et al. 2014). Such novae are thus also symbiotic stars, a spectroscopic definition of an interacting binary with a hot component and a cold, luminous one (a red giant, supergiant or AGB star). Symbiotics usually contain an accreting compact object, a white dwarf in the vast majority of cases.

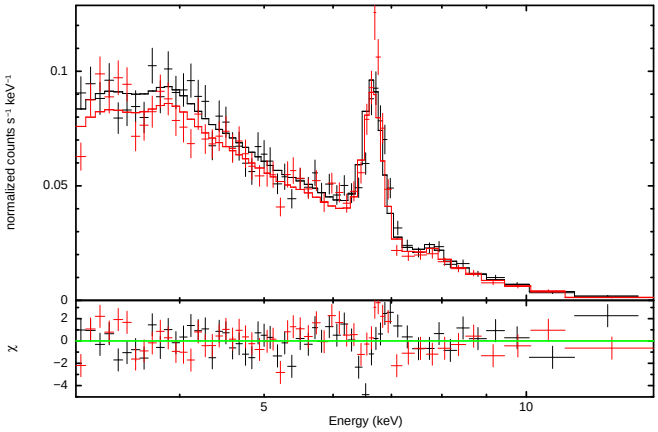

Figure 1. The X-ray spectrum of V745 Sco obtained with the NuSTAR FPMA (black) and FPMB (red) modules. The 3-10 keV range where most of the flux is emitted is shown in this plot. The fit shown is with the parameters of the first model in Table 2.

V745 Sco is the fastest Galactic nova. Three outbursts were observed in 1937, 1989 and 2014, all characterized by a very rapid decline of the light curve (t_2=2 day and t_3=4 days were the times to decay by 2 and 3 magnitudes, respectively, in the AAVSO light curves of 2014). Each time the ejecta expanded at very high velocity (Duerbeck 1989; Banerjee et al. 2014). Because the outbursts evolved so rapidly, we cannot rule out that they occur more frequently and have not been observed each time. Dürbeck (1989) described the 1989 outbursts and classified the nova as a symbiotic system because of the TiO bands, clearly detected already in outburst, which are typical of an M6 III spectral type. In subsequent observations in quiescence the secondary was classified in the range M6±2 III, depending on indicators in the infrared and optical spectrum (see brief review by Banerjee et al. 2014). V745 Sco was observed in X-rays in quiescence in 2010, and appeared as a faint, absorbed X-ray source (Luna et al. 2014). Despite poor statistics, Luna et al. (2014) performed a "tentative fit" with an absorbed optically thin thermal plasma at temperature kT >10 keV and N(H)>1.5 $\times 10^{21}$ cm^{-2} and attributed the X-ray emission to a disk boundary layer.

Already at the beginning of the outburst, long before the nebular phase, a strong and broad [O III] line was detected in the optical spectrum at 5007 Å. This line seems to be clearly associated with the red giant wind and not with the nova outflow (Duerbeck 1989). A [Fe II] line was present from the beginning, and within two weeks the nova showed a coronal spectrum with other strong coronal lines of high excitation potential, including [Fe VII], [Fe X], [Fe XI], [Fe XIV], and [Ni XII]. The early evolution after the discovery on 2014, February 6, (R. Stubbings, AAVSO special notice no. 380) has been described in a number of Astronomer's Telegrams (see e.g. Anupama et al. 2014; Page et al. 2014; Rupen et al. 2014). Banerjee et al. (2014) have described the development of the infrared spectrum: the ejecta initial velocity exceeded 4000 km s^{-1}, and there was no "free expansion stage", but only a Sedov-Taylor expansion, indicating a violent shock at the beginning of the outburst, in a region of high density material already present before the explosion.

Fermi detected the nova in gamma rays at a 2 and 3

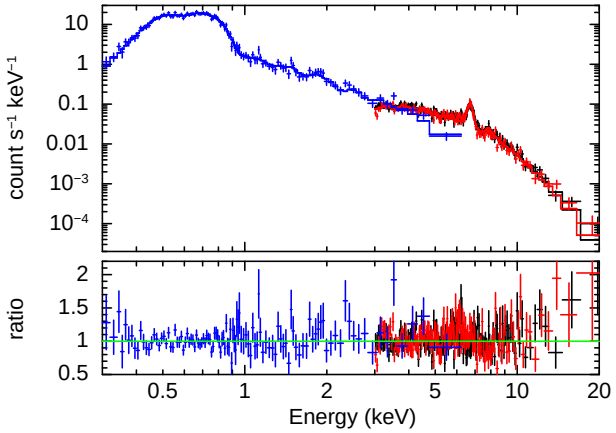

Figure 2. X-ray spectra of V745 Sco obtained with NuSTAR (3-20 keV) and with the Swift XRT (0.3-10 keV), fitted with the model in the second column of Table 2.

σ level on the first day after the outburst was announced (Cheung et al. 2014). Hard X-rays were also observed with Swift on the same day, and could be fitted with a thermal spectrum with kT$\simeq$8 keV (Mukai et al. 2014).

3 THE *NUSTAR* OBSERVATION

V745 Sco was observed with *NuSTAR* 10 days after the announced optical discovery on 2014 February 16 at 00:51:07 UT in a net, not continuous exposure lasting 22.5 kiloseconds, ending at 12:51:07 UT. *NuSTAR*, the first focusing hard X-ray telescope in 3-79 keV energy range, consists of two co-aligned telescopes with two focal planes, FPMA and FPMB (Harrison et al. 2013). The data were processed and screened using the standard pipeline for on-axis point sources (NUPIPELINE) in the *NuSTAR* Data Analysis Software (NUSTARDAS) version 1.3.1, recently included in the HEASOFT distribution. The *NuSTAR* calibration database (CALDB) version 20131223 was used throughout the analysis. The light curves and the spectra were extracted from the cleaned event files using NUPRODUCTS tool. The source photons were extracted from a circular region centered on the source position with a radius of 60 arcsec. A detailed background model for the source position in each of the two *NuSTAR* telescopes was derived by using the nuskybgd tool (Wik et al. 2012) to fit blank sky regions covering the entire field of view for each focal plane. This is more accurate than the usual method of simply scaling from the background of a nearby blank sky region, especially for faint sources, because it correctly accounts for gradients across the detectors.

By the time of the *NuSTAR* observation, the central supersoft X-ray source was the dominant source of X-ray flux (see e.g. Page et al. 2014b), but it is not observable in *NuSTAR*'s bandpass. The count rates measured with the two telescopes in different ranges are reported in Table 1. A luminous source was detected up to about 20 keV, and above this energy the observation is dominated by the background. The flux was 1.68$\pm$0.10 $\times$ 10^{-11} erg cm^{-2} s^{-1} in the 3-20 keV range. The upper limit for the flux in the 20-70 keV range is $\simeq$ 10^{-13} erg cm^{-2} s^{-1}.

We clearly detect the unresolved iron He-like triplet at 6.73$\pm$0.02 keV, with an equivalent width of about 1 keV.

Table 1. Count rate measured with the fpma and fpmb telescopes in the whole NuSTAR range, and in the "soft" sub-ranges 3-10 keV, 3-10 keV, 10-20 keV.

Range (keV)	FPMA cts/s	FPMB cts/s
3-79	0.3354$\pm$0.0040	0.3158$\pm$0.0039
3-20	0.3349$\pm$0.0039	0.3154$\pm$0.0038
3-10	0.3241$\pm$0.0038	0.3046$\pm$0.0037
10-20	0.0095$\pm$0.0007	0.0098$\pm$0.0007

We show in the next Section that the flux and plasma temperature are consistent with those derived analysing a Swift observation done while the *NuSTAR* exposures were ongoing (observation id. 00033136033), however, the *Swift* spectrum in the SSS phase requires an extremely hot and luminous stellar atmosphere, which cannot be observed at all in the *NuSTAR* range.

4 SPECTRAL FITS AND ADDITIONAL SWIFT DATA

A fit to the NuSTAR spectrum is shown in Fig. 1 and Table 2, using an XSPEC "VAPEC" model of plasma in collisional ionization equilibrium at kT=2.66 keV, flux 1.6 $\times 10^{-11}$ erg cm^{-2} s^{-2} and iron abundance [Fe/Fe$_\odot$]=0.51. This best fit yields a reduced χ^2 value of 1.3. We were not able to obtain a better fit with different models, even by adding more model components. From the emission measure fit we can obtain the average electron density of the ejecta emitting the X-rays, by making an assumption about the distance traveled by the ejecta. The work of Banjeree et al. (2014) is very useful, because these authors measured the velocity on different dates. They comment that the velocity law can be fitted with a third degree polynomial law, but they do not specify how their fit in their figure 3 was obtained. To find the range of interest of the electron density we can simply assume that radius of an idealized spherical shell would be smaller that reached with the initial epansion velocity (4825 km s^{-1}), but larger than reached with the velocity at day 10.3 (the time of the *NuSTAR* observation, that is 1930 km s^{-1}. We thus obtain a value of n$_e$ between 4.7 $\times 10^6$ cm^{-3} and 7.4 $\times 10^7$ cm^{-3}. This range is only indicative of the average value, and is obtained with the assumption that the flux was emitted in a spherical shell around the WD, of homogeneous density. The corresponding mass of the ejecta, if the hard X-ray emission region represents all the ejected mass, would be 5 $\times 10^{-8}$ M$_\odot$. We note that a power law component does not improve the fit, and clearly the data cannot be well fitted with a power law. The prominence of the iron feature is only due to the sensitivity of *NuSTAR* in the range around 7 keV, but the iron abundance we obtained from the best fit is only [Fe/Fe$_\odot$=0.51. We kept this abundance value fixed in the other fits described below.

Swift data were taken at semi-regular intervals of half a day or less, and those obtained just a few hours before the *NuSTAR* exposure (2014 February 16 1:35:17 UT for an exposure time of 1038 s, observation 00033136033) explain the difficulty in finding an optimal fit: the central source is more luminous than the nova shell and the lower limit of

Table 2. Fitting models and parameters for the *NuSTAR* and *Swift* observations separately and together. The columns with the asterisk indicate the addition of the two oxygen emission features. All the fluxes (absorbed in the 0.3-1 keV, specific flux of each XSPEC VAPEC model component of plasma in collisional ionization equilibrium, c1 and c2, absorbed flux in the whole range used for the fit, and unabsorbed total flux), are in units of erg cm^{-2} s^{-1}. Component c1 is the one mainly observed with *NuSTAR*.

Parameter	*NuSTAR* 3-10 keV	*Swift* 0.3-10 keV	*Swift** 0.3-10 keV	*Swift* & *NuSTAR* 0.3-79 keV	*Swift* & *NuSTAR* * 0.3-79 keV
N(H) (10^{21} cm^{-2})	$1.15^{+0.94}_{-0.12}$	$8.7^{+1.2}_{-0.3}$	$6.8^{+1.3}_{-1.1}$	8.0±0.4	6.9±0.9
kT$_{c1}$ (keV)	$2.66^{+0.09}_{-0.14}$	$1.62^{+0.14}_{-0.11}$	$2.77^{+0.87}_{-0.50}$	$2.76^{+0.07}_{-0.10}$	$2.76^{+0.08}_{-0.10}$
kT$_{c2}$ (keV)		$0.068^{+0.001}_{-0.013}$	$0.86^{+0.12}_{-0.16}$	$0.83^{+0.11}_{-0.12}$	$0.87^{+0.12}_{-0.13}$
Fe/Fe$_\odot$	0.51	0.51	0.51	0.51	0.51
T$_{\rm eff}$ (10^5 K)		$9.81^{+0.04}_{-0.06}$	10.0±0.2	9.79±0.04	$10.0^{+0.2}_{-0.1}$
F(0.3-1 keV)		1.71×10^{-10}	1.81×10^{-10}	1.66×10^{-10}	1.81×10^{-10}
F$_{c1}$	1.60×10^{-11}	4.02×10^{-11}	3.95×10^{-11}	2.97×10^{-11}	3.04×10^{-11}
F$_{c2}$		4.31×10^{-11}	1.70×10^{-11}	1.91×10^{-11}	1.90×10^{-11}
F$_{\rm tot}$	1.60×10^{-11}	2.11×10^{-10}	2.26×10^{-10}	2.16×10^{-10}	2.39×10^{-10}
F$_{\rm tot,u}$	1.62×10^{-11}	3.66×10^{-8}	3.66×10^{-8}	7.39×10^{-8}	3.81×10^{-8}
χ^2/d.o.f.	1.3	2.3	1.06	1.6	1.3

the *NuSTAR* bandpass is higher than the energy at which most of the X-rays are emitted. The soft part of the spectrum is very luminous and probably due to more than one emission mechanism, so the range around 3 keV is not well constrained. The full *Swift* dataset describing the nova evolution with snapshot exposures taken even three times a day is being analysed by the *Swift* team with several coauthors (Page et al. 2014c, in preparation), but here suffice it to say that we checked two additional exposures taken a few hours after the *NuSTAR* one and did not find significant spectral evolution in this short time. The large luminosity of the supersoft source (see Fig. 2) is still below a critical threshold of about 50 cts s^{-1} that may cause pile-up for the supersoft sources in *windowed timing mode*, used for this observation. In Table 2 we report the results of two fits of the *Swift* spectrum of this observation. In the first one we used a stellar atmosphere at 930,000 K (Rauch 2010, model), a low temperature plasma VAPEC model component in XSPEC at 68 eV, and a third a component, VAPEC at about 1.6 keV, obtaining a value 2.3 for the reduced χ^2. We cannot improve the fit with additional components, but it improves by using a blackbody with an oxygen absorption edge at 0.87 keV of arbitrary depth. An even better fit was obtaining by superimposing additional emission features of oxygen on the VAPEC models, H-like Lyman α at 0.65 keV and a blended He-like triplet at 0.57 keV. The fit results statistically acceptable, with $\chi^2 = 1.1$. The total flux is 2.26×10^{-10} erg cm^{-2} s^{-1}, largely due to the supersoft source, with an unabsorbed flux 3.66×10^{-8} erg cm^{-2} s^{-1}. The physical reason behind the need to add these "artificial" features is not due to an unusually high oxygen abundance in the plasma component. We did not have available grids of atmospheric models with a lower oxygen abundance, so that the oxygen absorption features were too deep and needed to be "corrected". Since atmospheric models with appropriate abundances are not available yet, we resorted to this arbitrary addition.

The best fit to the *Swift* and the *NuSTAR* spectra together is shown in Fig. 2, with the parameters in Table 2. We can constrain the hotter component and the value of N(H) using both sets of X-ray telescopes, and obtain N(H)=(6.9±0.9) $\times$ 10^{21} cm^{-2}, while the hot plasma has kT=2.76 keV. We note that N(H) is higher than the value $\simeq 4.8\times10^{21}$ cm^{-2} that one would expect applying e.g. the relationship derived by Güver & Özel (2009) to the interstellar reddening E(B-V)=0.7 given in Banerjee et al. (2014), impling a certain amount of intrinsic absorption, likely due to the red giant wind.

5 CONCLUSIONS

The observation of the very fast RN V745 Sco with *NuSTAR* 10 days after the discovery of the optical outburst and the observed maximum indicates that the hard X-ray emitting region at this stage had already cooled. We rule out plasma components hotter than 2.8 keV. Hard X-ray emission due to Comptonized gamma rays can also be ruled out because it would produce a power law spectrum with copious flux above 20 keV (e.g. Livio et al. 1992), which was not observed in the high energy band of *NuSTAR*.

The threshold detection flux of Fermi is of the order of 10^{-10} erg cm^{-2} s^{-1}, so we do not know whether there was gamma-ray emission with flux below this level, but hard X-rays are also an important indicator of gamma rays because the flux due to Comptonized down-scattered photons should be measurable. The optical depth of Compton scattering is

$$t_{\rm e} = n_{\rm e}\sigma_\tau {\rm D},$$

where n$_{\rm e}$ is the electron density and the Thomson cross section is σ_τ=6.6524 $\times10^{-25}$ cm^2. Adopting n$_{\rm e}$ $\simeq$ $\times10^7$ cm^{-3} derived above, and assuming that the photons have to cross a region of depth D as large as the distance to which the ejecta at have expanded in 10 days. Given the range of velocities from the first and tenth day (Banerjee et al. 2014, see above), 1.7×10^{14} cm$<$D$<$ 4.2×10^{14} cm, so we derive t$_{\rm e}$ to be in the range 1.1-2.8 $\times10^{-3}$. Optical depth t$_{\rm e} < 1$ indicates that the ejecta are optically thin to the Comptonized radiation, which should be clearly detectable for V745 Sco.

Do we have enough material in the shell to degrade the gamma-ray photons to X-rays with a significant Comptonized flux? Livio et al. (1992) calculated the X-ray light curve due to Comptonized gamma rays in the case of the

radioactive decay of ^{22}Na, at the specific fixed energy of the line at 1.22 MeV, which is two orders of magnitude lower than the lower range of the continuum gamma-ray emission of V745 Sco detected with Fermi. Despite the different gamma-ray range, these authors' Monte Carlo simulations should be relevant also for V745 Sco. In Livio et al. (1992) a peak of X-ray emission of order of one hundredth the value of the gamma-ray flux was predicted 200 days after the burst of gamma-ray emission, for ejecta with mass of 10^{-5} $M_{\odot}$ and a residual velocity of 10 km s^{-1}. The time to reach peak emission is directly proportional to the ejected mass and inversely proportional to its expansion velocity. Since the ejecta mass in a fast RN like V745 Sco is likely to be at least a factor of 10 lower than above, and the ejecta velocity after 10 days was still 200 times higher, a straightforward analogy would imply that the maximum emission of Comptonized X-rays for V745 Sco is expected within a few hours. The flux in our case should decay very quickly, like in the case analysed by Livio et al. (1992), peaking at a value around one hundredth the value of the gamma-ray flux. The upper limit for X-ray flux above 50 keV measured with *NuSTAR* is about 10^{-13} erg cm^{-2} s^{-1}, roughly translating into an upper limit estimate of the gamma ray flux 10 days after the outburst of V745 Sco of the order of 10^{-11} erg cm^{-2} s^{-1}.

We attribute the X-ray flux we measured with *NuSTAR* to shocks in the ejected shell, most likely as they impacted the red giant wind of the companion, like in the cases of V407 Cyg and RS Oph. We cannot tell at this stage whether the emission was due to the same region where the gamma rays originated on the first day, but it appears that in RN nova shells there are multiple regions of shocked material at different temperatures.

ACKNOWLEDGEMENTS

We wish to acknowledge the support of the following awards and funding agecies: M. Orio of ASI (Italian Space Agency) through an INAF-ASI grant, J.L. Sokoloski of the NSF award AST-1211778, and K.L. Page of the UK Space Agency funding the UK Swift Science Data Centre.

REFERENCES

Abdo A. A., Ackermann M., Ajello M., Atwood W. B., Baldini L., Ballet J., Barbiellini G., Bastieri D., Bechtol K., Bellazzini R., et al. 2010, Science, 329, 817

Anupama G. C., Selvakumar G., Moorthy V., Velu C., Dinakaran N., 2014, The Astronomer's Telegram, 5871, 1

Banerjee D. P. K., Joshi V., Venkataraman V., Ashok N. M., Marion G. H., Hsiao E. Y., Raj A., 2014, ApJ, 785, L11

Bode M. F., O'Brien T. J., Osborne J. P., Page K. L., Senziani F., Skinner G. K., Starrfield S., Ness J.-U., Drake J. J., Schwarz G., Beardmore A. P., Darnley M. J., Eyres S. P. S., Evans A., Gehrels N., Goad M. R., Jean P., Krautter J., Novara G., 2006, ApJ, 652, 629

Cheung C. C., Jean P., Shore S. N., 2014, The Astronomer's Telegram, 5879, 1

Duerbeck H. W., 1989, The Messenger, 58, 34

Güver T., Özel F., 2009, MNRAS, 400, 2050

Livio M., Mastichiadis A., Oegelman H., Truran J. W., 1992, ApJ, 394, 217

Lloyd H. M., O'Brien T. J., Bode M. F., Predehl P., Schmitt J. H. M. M., Truemper J., Watson M. G., Pounds K. A., 1992, Nature, 356, 222

Luna G. J. M., Pillitteri I., Mukai K., Sokoloski J. L., 2014, The Astronomer's Telegram, 5881, 1

Martin P., Dubus G., 2013, A&A, 551, A37

Metzger B. D., Hascoët R., Vurm I., Beloborodov A. M., Chomiuk L., Sokoloski J. L., Nelson T., 2014, MNRAS, 442, 713

Mróz P., Poleski R., Udalski A., Soszyński I., Szymański M. K., Kubiak M., Pietrzyński G., Wyrzykowski Ł., Ulaczyk K., Kozłowski S., Pietrukowicz P., Skowron J., 2014, MNRAS, 443, 784

Mukai K., Ishida M., 2001, Apj, 551, 1024

Mukai K., Page K. L., Osborne J. P., Nelson T., 2014, The Astronomer's Telegram, 5862, 1

Nelson T., Chomiuk L., Roy N., Sokoloski J. L., Mukai K., Krauss M. I., Mioduszewski A. J., Rupen M. P., Weston J., 2014, ApJ, 785, 78

Nelson T., Orio M., Cassinelli J. P., Still M., Leibowitz E., Mucciarelli P., 2008, Apj, 673, 1067

Ness J.-U., Starrfield S., Jordan C., Krautter J., Schmitt J. H. M. M., 2005, MNRAS, 364, 1015

Orio M., 2012, Bulletin of the Astronomical Society of India, 40, 333

Orio M., Behar E., Gallagher J., Bianchini A., Chiosi E., Luna G. J. M., Nelson T., Rauch T., Schaefer B. E., Tofflemire B., 2013, MNRAS, 429, 1342

Orio M., Parmar A., Benjamin R., Amati L., Frontera F., Greiner J., Ögelman H., Mineo T., Starrfield S., Trussoni E., 2001, MNRAS, 326, L13

Page K. L., Osborne J. P., Beardmore A. P., Mukai K., 2014, The Astronomer's Telegram, 5870, 1

Rohrbach J. G., Ness J.-U., Starrfield S., 2009, AJ, 137, 4627

Rupen M. P., Mioduszewski A. J., Chomiuk L., Sokoloski J., Nelson T., Mukai K., 2014, The Astronomer's Telegram, 5884, 1

Sekiguchi K., Whitelock P. A., Feast M. W., Barrett P. E., Caldwell J. A. R., Carter B. S., Catchpole R. M., Laing J. D., Laney C. D., Marang F., van Wyk F., 1990, MNRAS, 246, 78

Sokoloski J. L., Luna G. J. M., Mukai K., Kenyon S. J., 2006, Nature, 442, 276

Sokoloski J. L., Mukai K., Luna G. J. M., 2006, The Astronomer's Telegram, 737, 1

Sokoloski J. L., Rupen M. P., Mioduszewski A. J., 2008, ApJ, 685, L137

Tofflemire B. M., Orio M., Page K. L., Osborne J. P., Ciroi S., Cracco V., Di Mille F., Maxwell M., 2013, ApJ, 779, 22

Williams R., 2013, AJ, 146, 55

Williams R. E., Hamuy M., Phillips M. M., Heathcote S. R., Wells L., Navarrete M., 1991, ApJ, 376, 721